Multimodality Imaging in Hypereosinophilic Syndrome With Cardiac Involvement

Karuppiah Arunachalam, MD, Charles Beale, MD, Eirini Apostolidou, MD, Michael Atalay, MD, Daniel Levine, MD, Karen Aspry, MD, and Rayan Yousefzai, MD, *Providence, Rhode Island*

INTRODUCTION

Eosinophilic granulomatosis with polyangiitis (EGPA), previously known as Churg-Strauss syndrome, is a vasculitis of small and medium-sized vessels characterized by extravascular granulomas, eosinophilia, and tissue infiltration by eosinophils. It usually presents with allergic rhinitis and adult-onset asthma. The most commonly involved organ is the lung, followed by the skin. Involvement of extrapulmonary organs is largely responsible for the morbidity and mortality associated with EGPA, with cardiac involvement being the primary contributor to mortality. We present a case of EGPA with cardiac involvement in which multimodality imaging was used for accurate diagnosis and early therapy.

CASE PRESENTATION

The patient was a 53-year-old man with a history of asthma and environmental allergies who was referred to the emergency department by his ophthalmologist after presenting with sudden-onset blurred vision in the left eye and evidence of optic neuritis. He endorsed a 2-week history of night sweats, weakness, fatigue, arthralgias, anorexia, transient ankle edema, and a rash involving the hands and feet, with minimal associated pruritus. He denied intravenous drug use, recent travel, exposure to pets, and family history of autoimmune disease.

On presentation, body temperature was 99.4°F, blood pressure was 111/79 mm Hg, heart rate was 95 beats/min, and oxygen saturation was 96%. The patient's examination was notable for purpuric lesions of the hands and feet and left temporal and nasal visual field deficits. On dilation of his left eye, optic disk edema was present. Furthermore, he demonstrated mildly elevated jugular veins, crackles at the bases of the lungs, and mild bilateral lower extremity edema.

Laboratory data were significant for a white blood cell count of 36,000 cells/mm^3 with 69% eosinophils, a C-reactive protein level of 63 mg/dL, an erythrocyte sedimentation rate of 122 mm/min, an elevated immunoglobulin E level of 1,741 IU/mL, a troponin level of 11 ng/mL, and a brain natriuretic peptide level of 790 pg/mL. Results of infectious workup including human immunodeficiency virus antibody/antigen, *Anaplasma phagocytophilum*, *Ehrlichia chaffeensis*, *Babesia microti*, and *Bartonella* antibodies, bacterial and fungal blood cultures, Lyme reflex, and blood parasite smear were negative. Results of rheumatologic workup including anticardiolipin antibodies, lupus anticoagulant, antinuclear antibodies, antineutrophil cytoplasmic antibody, and C3 and C4 complement levels were within normal limits. Electrocardiography showed low voltage in limb leads and q waves in anteroseptal leads (Figure 1).

Magnetic resonance imaging of the brain revealed acute punctate infarcts within the right centrum semiovale, right frontal, and right parieto-occipital lobes. Transthoracic echocardiography revealed a mildly dilated left ventricle with end-diastolic diameter measured at 60 mm with global hypokinesis and severely reduced systolic function (ejection fraction 30%) and thinning of the septum. A small pericardial effusion was noted without evidence of tamponade physiology (Figures 2 and 3, Videos 1 and 2). Mild mitral regurgitation without other significant valvular disease was present. Echocardiography also showed abnormal findings on Doppler tissue imaging with low early diastolic mitral annular velocity (e′) measured at 8 cm/sec (Figure 4), ratio of early mitral inflow velocity to early diastolic mitral annular velocity (E/e′) of 14.5, and abnormal strain pattern with global longitudinal strain of −10.89% (Figure 5).

Cardiac catheterization showed normal coronary arteries, mildly elevated filling pressures, and normal cardiac output (right atrial pressure 11 mm Hg, pulmonary artery pressure 43/25 mm Hg with a mean of 31 mm Hg, pulmonary capillary wedge pressure 25 mm Hg, and cardiac index 2.8 L/m^2).

Cardiac magnetic resonance (CMR) with gadolinium and T1 mapping before and after gadolinium for tissue characterization was performed and showed moderate to severe biventricular dysfunction, patchy biventricular subendocardial late gadolinium enhancement, and a small pericardial effusion (Figure 6, Video 3). On the basis of these findings, the patient underwent endomyocardial biopsy, which showed increased perivascular eosinophils and eosinophilic degranulation and fibrin (Figure 7).

Even though bone marrow biopsy is not necessary for the diagnosis of the EGPA, it was performed to rule out malignancy. The results showed hypereosinophilia (Figure 8), without evidence of malignancy, confirming the diagnosis of EGPA given the patient's history of allergic rhinitis and asthma. He was started on high-dose steroids and cyclophosphamide, which rapidly resolved his eosinophilia within 48 hours. The blurred vision resolved immediately in response to the immunosuppression therapy. Even though the blurred vision could have been related to a thromboembolic event, he was not started on anticoagulation. Blurred vision has been described in patients with EGPA. He completed a prolonged steroid taper, and repeat transthoracic echocardiography 7 weeks later showed significant improvement of left ventricular systolic function (ejection fraction 45%) with resolution of the pericardial effusion and end-diastolic diameter measured at 58 mm (Figures 9-11, Videos 4-6). After

From the Department of Internal Medicine (K.A.), the Department of Cardiology (C.B., E.A., D.L., K.A., R.Y.), and the Department of Radiology (M.A.), Warren Alpert Medical School of Brown University, Providence, Rhode Island.

Keywords: Hypereosinophilic syndrome, Echocardiography, Cardiac magnetic resonance

Conflicts of interest: The authors report no actual or potential conflicts of interest relative to this document.

2468-6441

https://doi.org/10.1016/j.case.2019.03.003

VIDEO HIGHLIGHTS

Video 1: Parasternal long-axis view revealing severely reduced left ventricular function (ejection fraction of 30%) with a mildly dilated left ventricle and a small pericardial effusion without temponade.

Video 2: Apical two-chamber view revealing severely reduced left ventricular function (ejection fraction of 30%) and normal left atrial size.

Video 3: Cardiac magnetic resonance showing moderate to severe biventricular dysfunction and a small pericardial effusion.

Video 4: Parasternal long-axis view revealing significant improvement of left ventricular systolic function (ejection fraction of 45%) with resolution of the pericardial effusion after immunosuppression therapy.

Video 5: Apical four-chamber view revealing significant improvement of the left ventricular function (ejection fraction of 45%) after immunosuppression therapy.

Video 6: Apical two-chamber view revealing significant improvement of the left ventricular function (ejection fraction of 45%) after immunosuppression therpay.

View the video content online at www.cvcasejournal.com.

immunosuppression therapy, Doppler tissue imaging with early diastolic mitral annular velocity (e′) measured at 12 cm/sec (Figure 12) and global longitudinal strain measured at −12.44% (Figure 13) have improved.

DISCUSSION

EPGA is a relatively rare vasculitis, which may involve the heart, but the diagnosis of cardiac involvement can be challenging. The differential diagnosis of hypereosinophilia with cardiac involvement includes EGPA, other hypereosinophilia syndromes with either idiopathic or known etiologies, eosinophilic leukemia, drug reactions, and parasitic infections. This case illustrates how clinical clues and multimodality imaging can lead to an earlier diagnosis and more timely treatment of EGPA with cardiac involvement. The latter is essential, because EGPA is likely underdiagnosed.[1] Cardiac manifestations are common (60%) and include electrocardiographic abnormalities, valvular insufficiency, pericardial effusion, left ventricular dysfunction, restrictive cardiomyopathy, pericarditis, and myocardial infarction.[2-4] Cardiac involvement in EPGA patients is associated with higher mortality and responsible for approximately 50% of the mortality associated with the disease.[5,6] In a case series of 383 patients with EGPA, 16% had cardiomyopathy and 15% had pericarditis.[3]

EGPA has a three-stage process of myocardial involvement.[7,8] Stage 1 is the acute necrosis stage due to eosinophilic infiltration and direct toxic effect. Stage 2 is the thrombotic stage due to thrombus formation in the endocardial surface. Stage 3 is the fibrotic stage as the result of the replacement of the injured myocardium by fibrotic tissue.

Patients with EGPA have a significantly increased risk for thromboembolic disease during the second stage of the disease. In a retrospective study of 232 patients with EPGA, the risk for thromboembolic disease was 8%.[9] Even though the most common cardiomyopathy associated with EGPA is restrictive cardiomyopathy, some patients can present with left ventricular dysfunction and abnormal myocardial relaxation without restriction,[2] and early therapy can prevent the fibrosis and developing restriction, as was the case with our patient.

Electrocardiographic abnormalities in patients with cardiac involvement are not well defined but have been reported to include repolarization changes manifested as pathologic q waves, as in our patient, as well as T-wave inversion, conduction abnormalities (right and left bundle branch block), and QT prolongation. QT prolongation is increased in cardiac involvement compared with the noncardiac group of patients with EGPA, but ventricular arrhythmias are rare despite higher QT prolongation.[10] Echocardiographic abnormalities may include systolic dysfunction with or without wall motion abnormalities, mural thrombi, valvular disease, and pericardial effusion, which was present in our patient.[11]

Rheumatologic investigation can also help narrow the diagnosis. A positive level of antineutrophil cytoplasmic antibody is associated with renal involvement, peripheral neuropathy, and biopsy-proven vasculitis, whereas a negative antineutrophil cytoplasmic antibody level may predict cardiac involvement, as in our patient.

CMR is an essential diagnostic tool and can reliably detects all stages of eosinophil-mediated heart damage, including the early stage of myocardial inflammation[12] to intracardiac thrombi and fibrosis, such as thickening of the valves' leaflets, and increases in endomyocardial echodensity in areas of fibrosis.[13] CMR is also correlates with eosinophilic infiltrates and hemorrhagic necrosis on endomyocardial

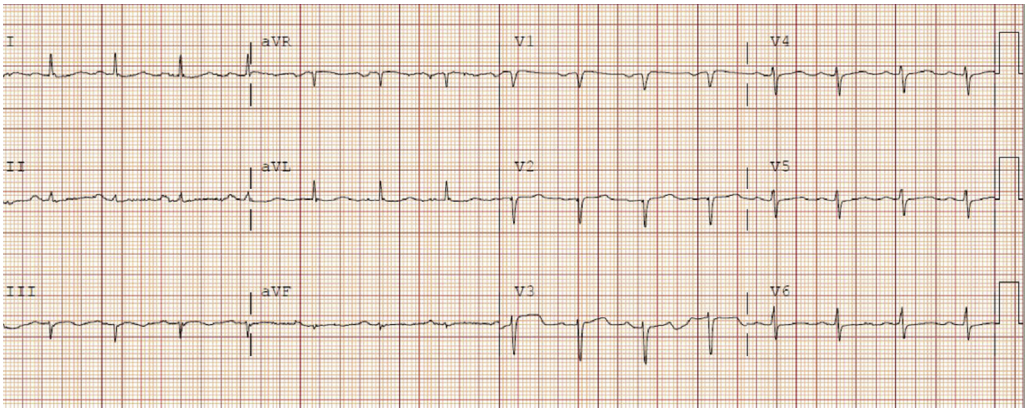

Figure 1 Electrocardiogram showing low voltage in limb leads and q waves in anteroseptal leads.

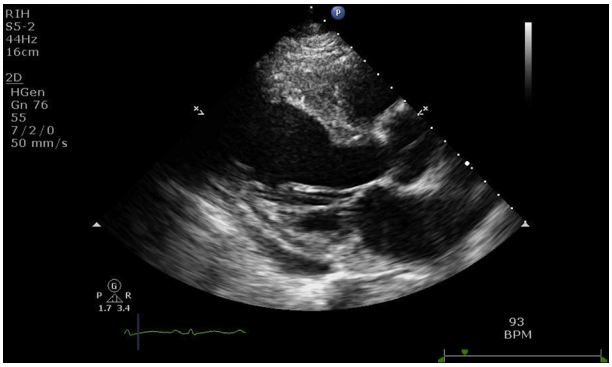

Figure 2 Parasternal long-axis view revealing a mildly dilated left ventricle with a small pericardial effusion.

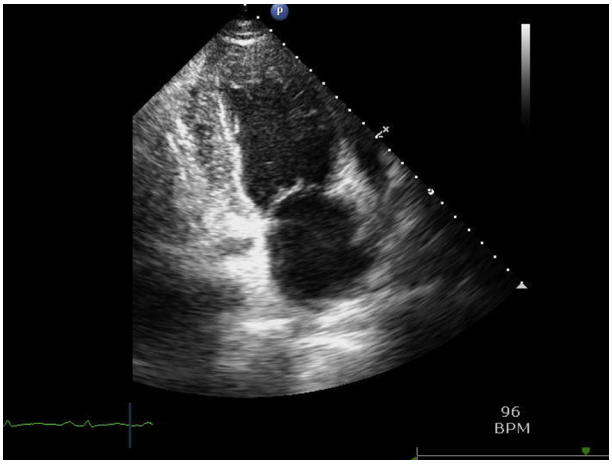

Figure 3 Apical two-chamber view revealing a mildly dilated left ventricle and normal left atrial size.

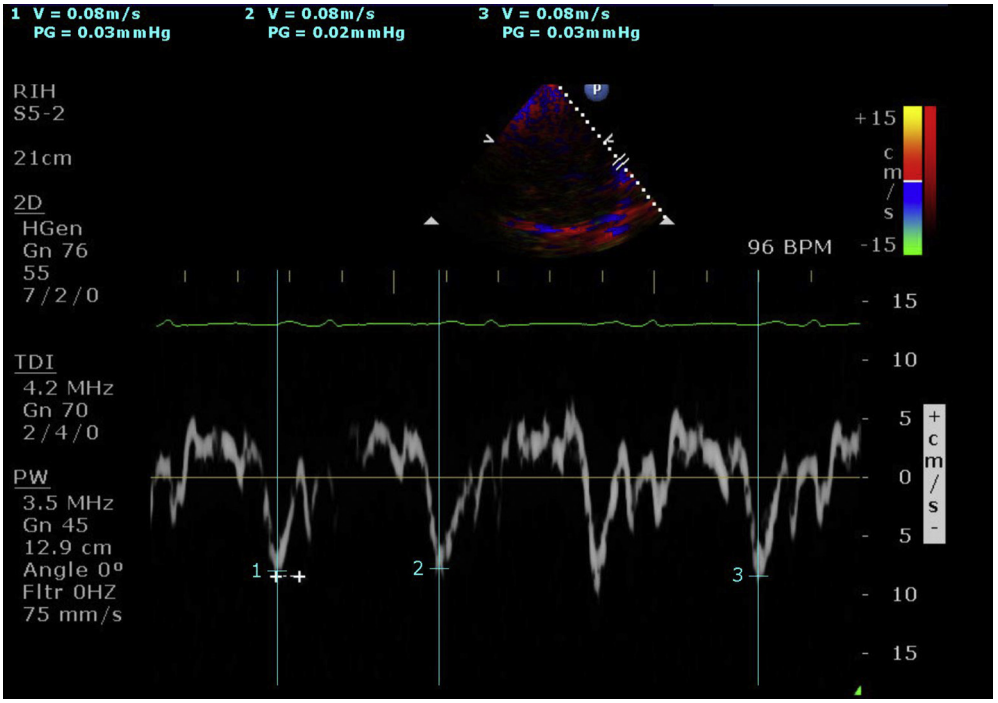

Figure 4 Tissue doppler imaging of lateral mitral annual velocity revealing a low early diastolic mitral annualr velocity of 8 cm/s.

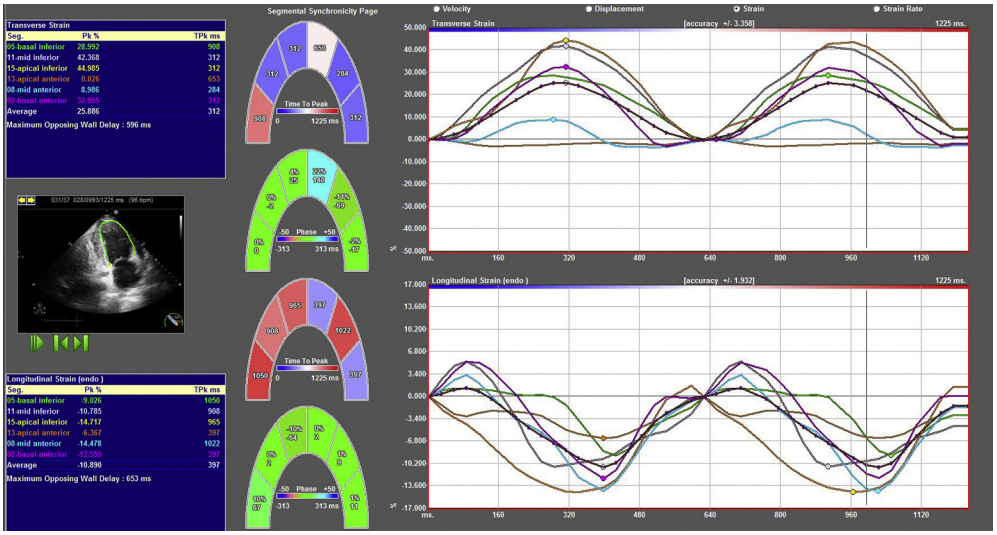

Figure 5 Strain imaging revealing an abnormal global longitudinal strain of −10.89.

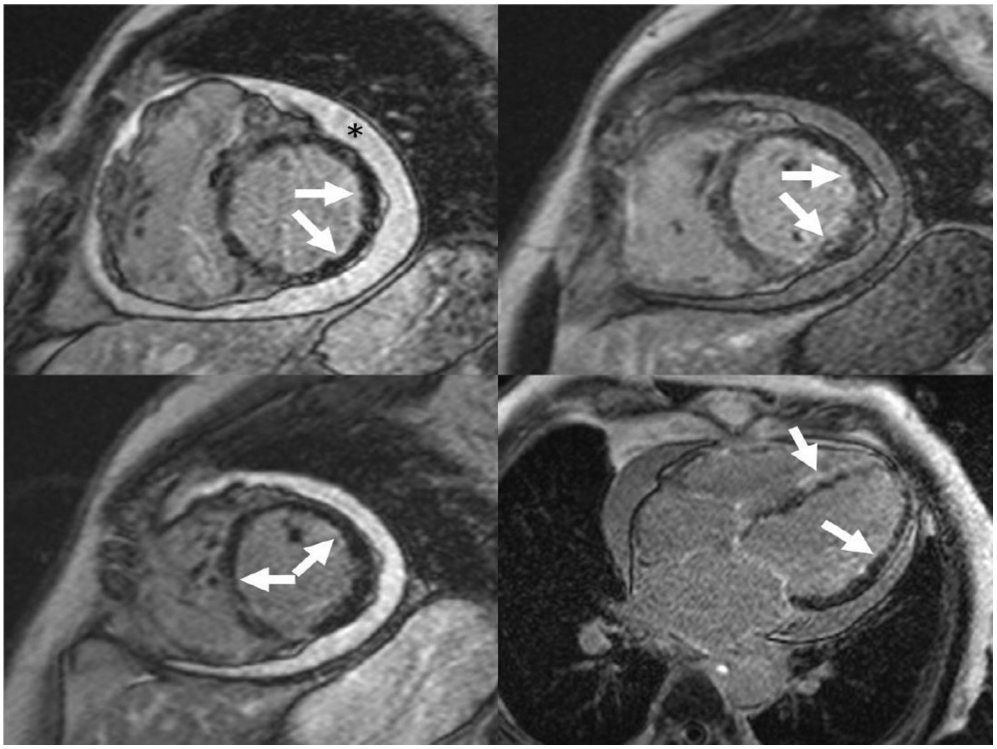

Figure 6 Cardiac magnetic resonance revealing moderate to severe biventricular dysfunction, a small pericardial effusion (*black asterisk*), and patchy biventricualr subendocardial enhancement (*white arrows*).

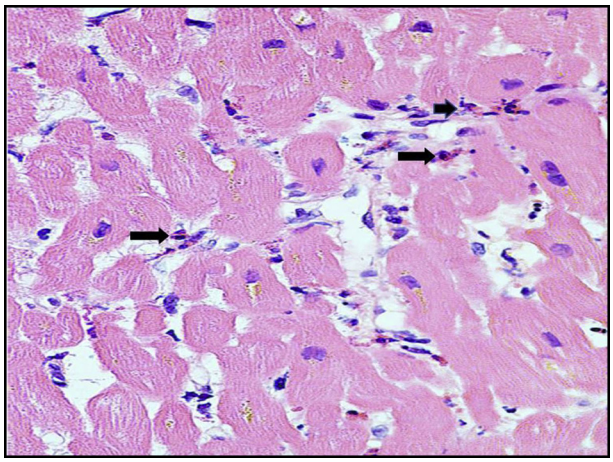

Figure 7 Endomyocardial biospy showing increased perivascular eosinophils/eosinophilic degranulation (*black arrows*) and fibrin.

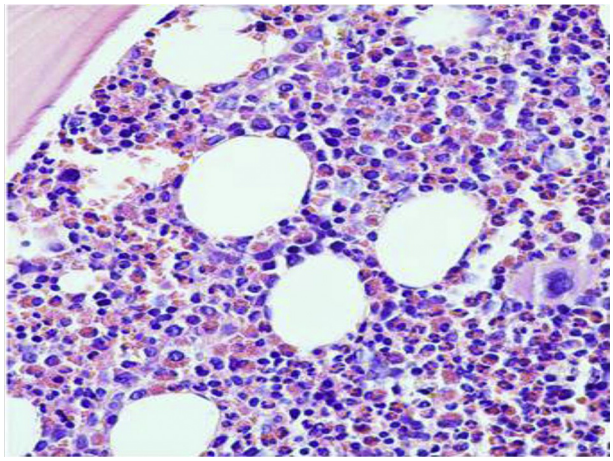

Figure 8 Bone marrow biopsy showing hypereosinophilia without evidence of malignancy.

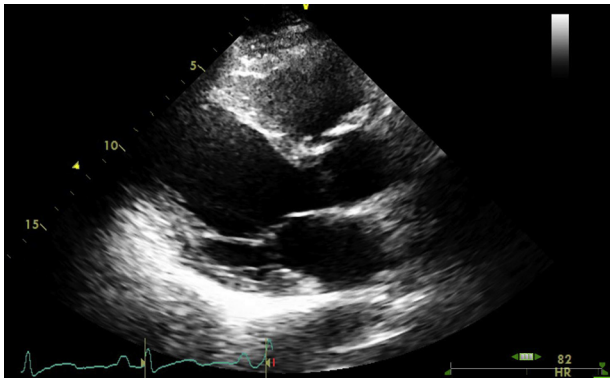

Figure 9 Parasternal long-axis view after immunosuppression therapy revealing normal left ventricualr size and resolution of the pericardial effusion.

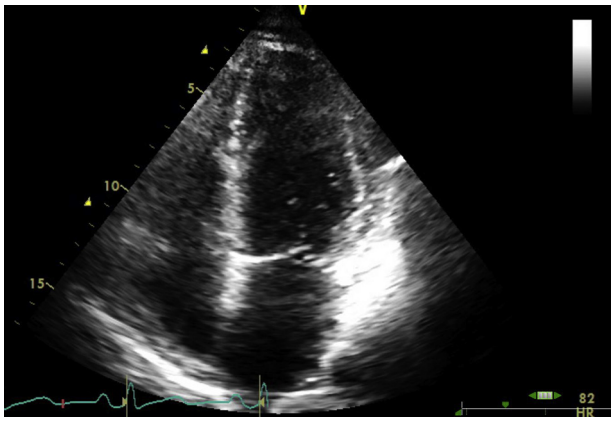

Figure 10 Apical four-chamber view after immunosuppression therapy revealing normal left ventricular size and normal atrial size.

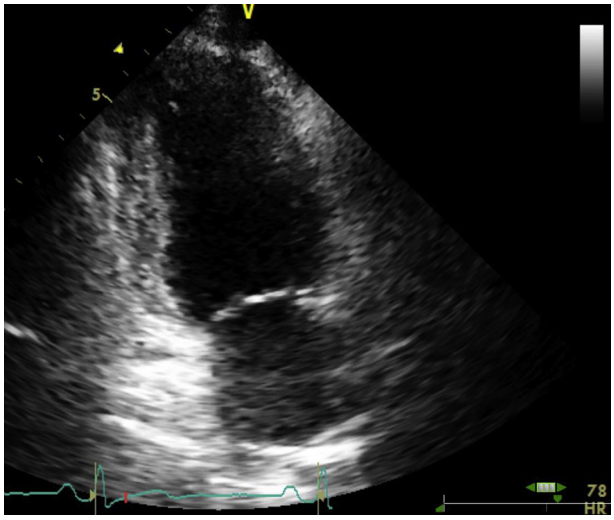

Figure 11 Apical two-chamber view after immunosuppression therapy revealing normal left ventricular size and normal left atrial size.

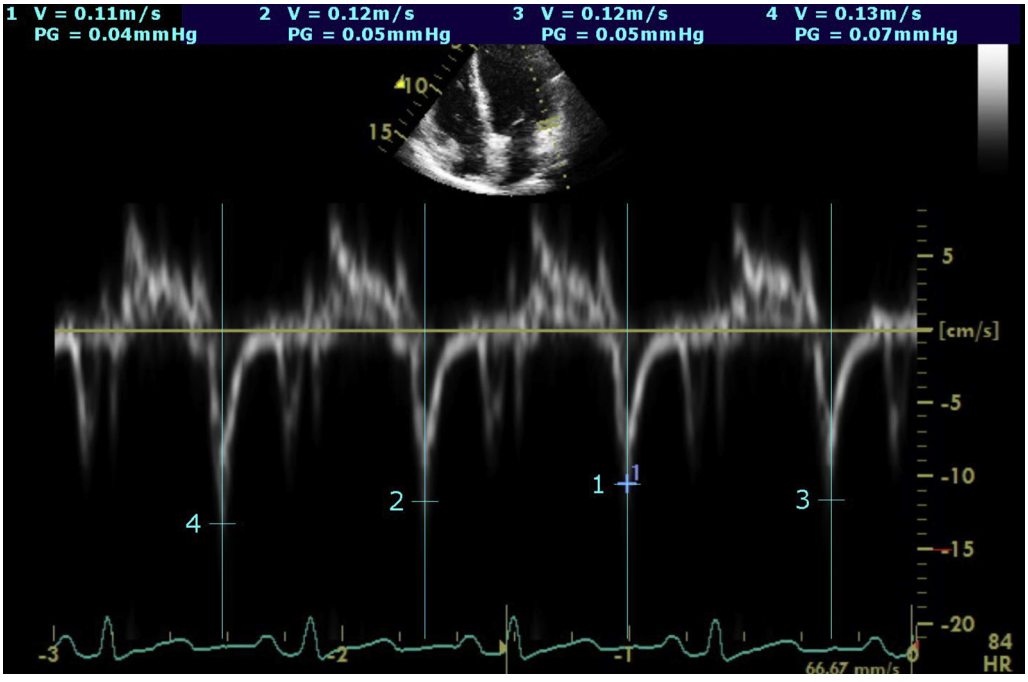

Figure 12 Tissue doppler imagimg of the lateral mitral annular velocity revealing improvement of early diastolic mitral annular velocity measured at 12 cm/s after immunosuppression therapy.

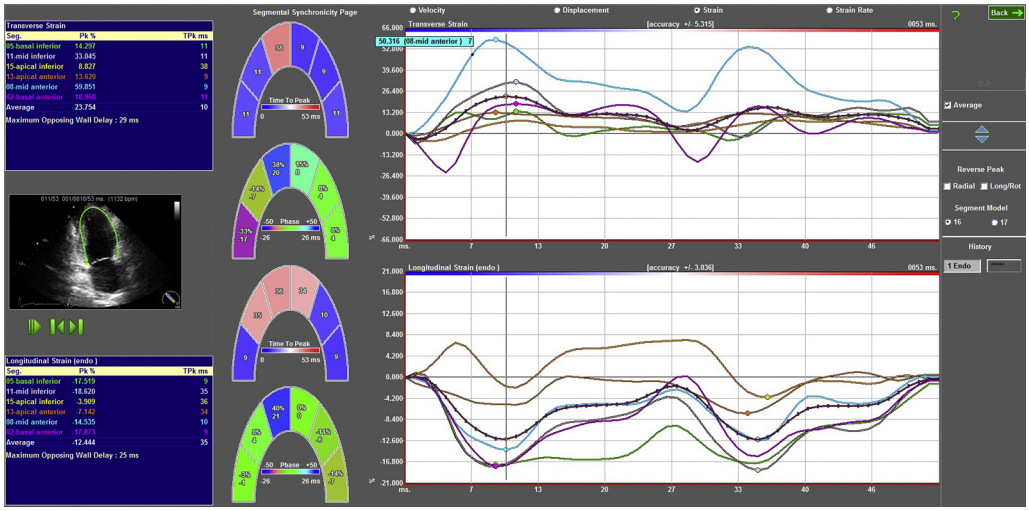

Figure 13 Strain imaging revealing an improvement of global longitudinal strain of −12.44 after immunosuppression therapy.

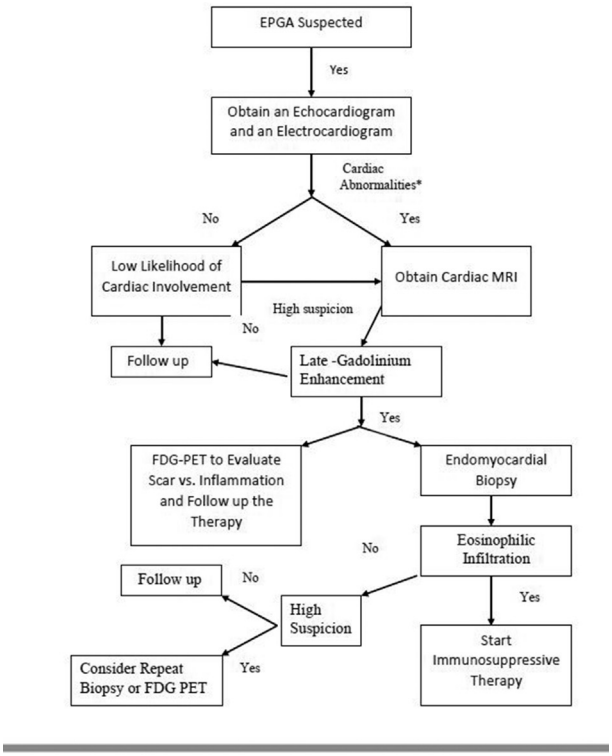

Figure 14 Diagnostic flow chart for the patients suspected with EPGA and cardiac involvement.

biopsy[14] and helps in assessing the involvement of pericardium. Fluoro-2-deoxyglucose positron emission tomography is another imaging modality used to assess whether delayed myocardial enhancement on CMR is due to fibrosis or inflammation.[15] It can also be used to follow the effectiveness of the therapy. An endomyocardial biopsy is performed when EGPA is suspected and typically reveals eosinophilic infiltration and endomyocarditis. Endomyocardial biopsy is essential for a definitive diagnosis and may be necessary for initiation of immunosuppressive therapy.[5]

EGPA is considered one of the reversible causes of left ventricular dysfunction, so prompt recognition and treatment are paramount. Figure 14 shows a diagnostic flowchart for patients suspected of having EPGA and cardiac involvement. Limited studies have shown that high-dose steroids and chemotherapy with cyclophosphamide are the most effective treatments for patients with EGPA and cardiac involvement. Patients with end-stage heart failure may require orthotopic heart transplantation, as some disease may be irreversible. Immunosuppressive treatment after transplantation is yet to be defined.

CONCLUSION

EPGA is a rare hypereosinophilic syndrome with cardiac involvement in up to 60% of patients and early development of myocardial fibrosis. Prompt recognition via multimodality imaging and endomyocardial biopsy, and rapid initiation of treatment with high-dose steroids and/or chemotherapeutic agents, may prevent progression or lead to recovery of cardiomyopathy.

SUPPLEMENTARY DATA

Supplementary data related to this article can be found at https://doi.org/10.1016/j.case.2019.03.003.

REFERENCES

1. Cottin V, Bel E, Bottero P, Dalhoff K, Humbert M, Lazor R, et al. Revisiting the systemic vasculitis in eosinophilic granulomatosis with polyangiitis (Churg-Strauss): a study of 157 patients by the Groupe d'Etudes et de Recherche sur les Maladies Orphelines Pulmonaries and the European Respiratory Society Taskforce on eosinophilic granulomatosis with polyangiitis (Chrug-Strauss). Autoimmun Rev 2017;16:1-9.

2. Brucato A, Maestroni S, Masciocco G, Ammirati E, Bonacina E, Pedrotti P. Cardiac involvement in Chrug-Strauss syndrome. G Ital Cardiol 2015;16:493-500.
3. Comarmond C, Pagnoux C, Khellaf M, Cordier JF, Hamidou M, Viallard JF, et al. Eosinophilic granulomatosis with polyangiitis (Churg-Strauss): clinical characteristics and long-term followup of the 383 patients enrolled in the French Vasculitis Study Group cohort. Arthritis Rheum 2013;65:270-81.
4. Bailey G, Upadhyaya K, Meadows J, Malm B. Eosinophilic myocarditis presenting as ST-segment elevation myocardial infarction diagnosed with cardiac magnetic resonance imaging. Am J Med 2016;129:e19-22.
5. Neumann T, Manger B, Schmid M, Kroegel C, Hansch A, Kaiser WA, et al. Cardiac involvement in Churg-Strauss syndrome: impact of endomyocarditis. Medicine (Baltimore) 2009;88:236-43.
6. Corradi D, Maestri R, Facchetti F. Postpartum Churg-Strauss syndrome with severe cardiac involvement: description of a case and review of the literature. Clin Rheumatol 2009;28:739-43.
7. Ten Oever J, Theunissen LJ, Trick LW, Verbunt RJ. Cardiac involvement in hypereosinophilic syndrome. Neth J Med 2011;69:240-3.
8. Kleinfeldt T, Nienaber CA, Kische S, Akin I, Turan RG, Korber T, et al. Cardiac manifestation of the hypereosinophilic syndrome: new insights. Clin Res Cardiol 2010;99:419-27.
9. Allenbach Y, Seror R, Pagnoux C, Teixeira L, Guilpain P, Guillevin L, et al. High frequency of venous thromboembolic events in Chrug-Strauss syndrome, Wegener's granulomatosis and microscopic polyangiitis but not polyarteritis nodosa: a systematic retrospective study on 1130 patients. Ann Rheum Dis 2009;68:564-7.
10. Szczeklik W, Sokołowska BM, Mastalerz L, Miszalski-Jamka T, Pacult K, Gorka J, et al. QT dispersion in patients with Churg-Strauss syndrome. Kardiol Pol 2011;69:1143-9.
11. Dennert RM, Van Paassen P, Schalla S, Kuznetsova T, Alzand BS, Staessen JA, et al. Cardiac involvement in Churg-Strauss syndrome. Arthritis Rheum 2010;62:627-34.
12. Debl K, Djavidani B, Buchner S, Poschenrieder F, Heinicke N, Feuerbach S, et al. Time course of eosinophilic myocarditis visualized by CMR. J Cardiovasc Magn Reson 2008;10:21.
13. Plastiras SC, Economopoulos N, Kelekis NL, Tzelepis GE. Magnetic resonance imaging of the heart in a patient with hypereosinophilic syndrome. Am J Med 2006;119:130-2.
14. Boccouche H, Yilmaz A, Alscher D, Klingel K, Val-Bernal JF, Mahrholdt H. Magnetic Resonance assessment and therapy monitoring of cardiac involvement in Chrug-Strauss syndrome. Circulation 2008;117:1745-9.
15. Marmursztejn J, Guilevin L, Trebossen R, Cohen P, Guilpain P, Pagnoux C, et al. Chrug-Strauss syndrome cardiac involvement evaluated by cardiac magnetic resonance imaging and positron-emission tomography: a prospective study on 20 patients. Rheumatology (Oxford) 2013;52:642-52.